

The Influence of particle Morphology on In-Flight Particle Velocity in Cold Spray

H. Fuknuma, N. OHno, B. Son, R. Huang
Plasma Giken Co., LTD., Toda City, Saitama, Japan

Abstract

Cold spray is a relatively recent spray coating technology in which a metal or alloy particle is plastically deformed by the kinetic energy of the particle accelerated in supersonic gas flow through a convergence and divergence nozzle when it impinges onto the substrate. The particle velocity at impact onto the substrate is a key factor to determine the characteristics of the cold spray deposit. Therefore, various researchs have been carried out on particle acceleration processes how to obtain faster particle velocity in cold spray. Mathematical modelings on particle acceleration in supersonic gas flow in Laval nozzle also have been made based on a spherical particle. From a view point how a non spherical particle behaves in supersonic gas flow, it was investigated experimentally that how particle morphology affects particle acceleration process in cold spray.

Two types of powder morphology were used for the experiment, the one was spherical and the other was angular and jagged. Those particle size distributions were almost the same. In-flight particle velocities of spherical and angular particles were measured with DPV-2000. It was found that the particle morphology greatly influenced the in-flight particle velocity and deposit efficiency.

Introduction

It is generally accepted that in cold spray, only the particle that exceeds a critical velocity can deposit on the substrate and the higher impact velocity brings higher deposition rates and better bonding strength. The characteristics of the deposit also significantly depends on the velocity[1, 2]. Therefore, the impact velocity is the most important factor in cold spray. The acceleration process of the particle in supersonic gas flow in a convergence and divergence nozzle has been investigate how to miximize the impact velocity.

Mathematical modelings on the particle acceleration process have been created on the basis of a spherical particle in the supersonic gas flow [3-6]. It has, however, not been clarified whether or not a non-spherical particle reaches higher velocity in supersonic gas flow. This paper presents how the particle morphology affects the in-flight particle velocity and critical velocity in supersonic gas flow in cold spray.

Materials and experimental procededures

The coating materials used for the experiments were stainless steel 316 L and bronze. Two types of powder morphology, spherical and angular, for each material were chosen from commercially available powders. The spherical and angular stainless steel powders were MicroMelt 316 L and FE-101 provided by Carpenter Technology Corporation (Wyomissing, PA USA) and Praxair Surface Technology Inc. (Indianapolis, IN USA) respectively. The spherical and angular bronze powders were Bro-Q and Bro-AtW respectively provided by Fukuda Foil & Powder Co., Ltd. (Yanashina, Kyoto, Japan).

The chemical compositions of the stainless steel and bronze powders are shown in table 1 and 2 respectively. Both

Table 1: The chemical compositions of the coating materials of stainless steel 316 L powders.

Component	Weight %	
	MicroMelt	FE-101
C	0.025	0.0244
Si	0.53	1
Mn	1.11	-
P	0.025	-
S	0.006	-
Ni	10.1	11
Cr	16.3	16
Mo	2.08	2
Fe	balance	balance

Table 2: The chemical compositions of the bronze powders.

Component	Weight %	
	Bro-Q	Bro-AtW
Sn	10.8	9.76
P	0.24	
Cu	balance	balance

chemical compositions of the stainless steel powders are almost same, although some of the components of FE-101 are not given in Table 1. Bro-Q powder contains a small amount of phosphorous but Bro-AtW does not include it. The content of tin is almost the same in both bronze powders.

The powder morphology of those metals is shown in Fig. 1. MicroMelt powder is spherical and has couple of small powders on some large particles, while FE-101 powder is angular and also has small particles on some large ones, and Bro-Q is spherical and Bro-AtW is angular as shown in Fig. 1.

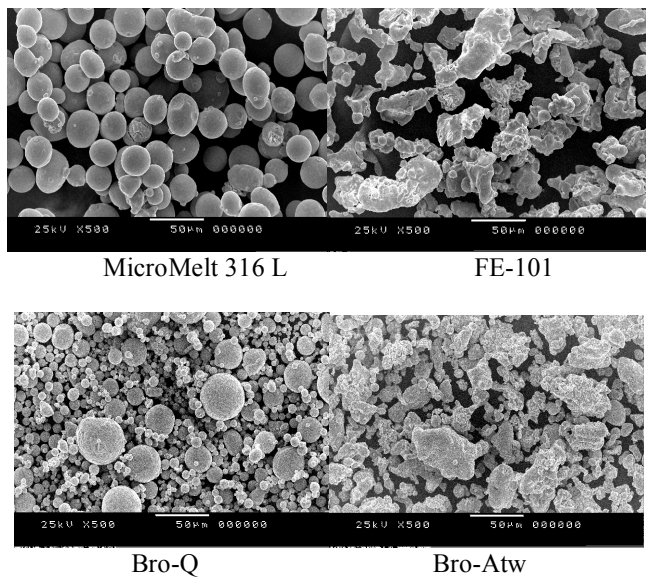


Fig.1: The SEM images of the stainless steel and bronze powders.

The particle size distributions of those four materials were measured with a laser diffraction particle analyzer, Mastersizer Model Type MAM5005, provided by Malvern Instrument Ltd. (Worcestershire, UK). The results are shown in Fig. 2. As for the stainless powders, the peaks of MicroMelt and FE-101 distribution curves are 29 and 34 µm respectively, and FE-101 curve is broader than MicroMelt one as shown in Fig. 2. FE-101 curve is broader and the peak is at 5 µm larger in particle size than MicroMelt. On the bronze powders, both distribution curves are similar and the peaks are 20 and 30 µm. Bro-Atw curve is shifted to 10 µm larger side from Bro-Q curve.

The particle hardness were measured with a micro-Vickers hardness tester. Ten particles of every powder were measured and the averages and standard deviations are shown in Table 3. As for the stainless powders, MicroMelt was harder than the twice of FE-101 particle hardness. Bro-Q was about 70 Hv harder than Bro-Atw.

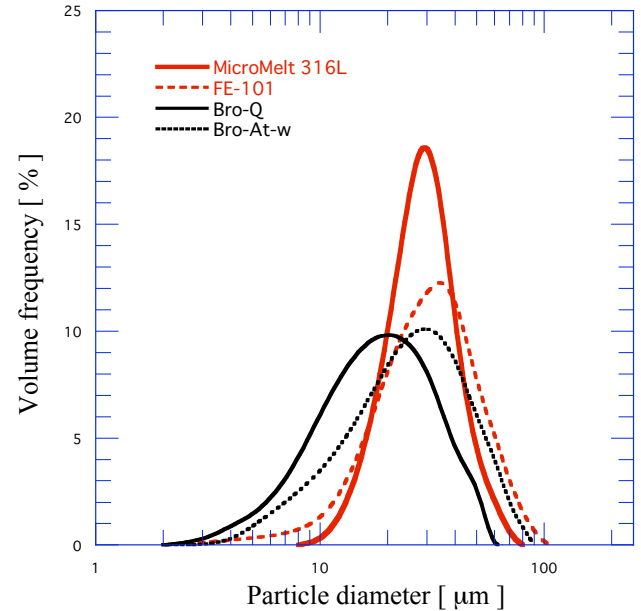


Fig. 2 The particle size distributions of the stainless steel 316 L and bronze powders.

Table 3: The particle hardness of the stainless steel 316 L and bronze powders.

	Average hardness [Hv]	Standard deviation
MicroMelt 316 L	332.8	29.5
FE-101	146.9	19.6
Bro-Q	190.6	18.4
Bro-Atw	122.0	32.6

The schematic illustration of the experimental setup for in-flight particle velocity measurements is shown with a cold spray touch, a in-flight particle velocity measurement sensor head and a laser generator in Fig. 3. The DPV-2000 system (Tecnor Automation Ltd., St-Bruno, QC, Canada) was modified to measure the velocity of cold particles. A laser beam generator was added to the system to obtain the light signals reflecting from the particle spotted by the laser beam because the light radiating from the cold particle less than 1300 K is too weak to be detected by the sensor. A mask was set on the tip of an optical fiber in the sensor head. When a particle flies in front of the mask, the signals from the particles pass through the two slits of the mask and the optical fiber to the detector. The in-flight particle velocity is determined by dividing the distance between the two slits by the time interval.

of the particle passing the slits. The particle size is also obtained to measure the energy from the particle.

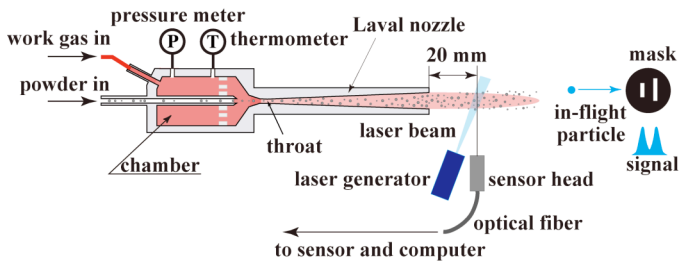


Fig. 3 The schinatic illustration of the experimental setup for measuring the in-flight particle velocity and particle sizes

The sensing head was placed to measure the small area at 20 mm from the nozzle exit in the nozzle center line. The laser beam of 780 nm wave length was generated to spot the area.

Table 4: The operating gas temperature and pressure conditions in cold spray of the stainless steel 316 L and bronze powders.

MicroMelt 316 L				
Chamber gas temperature	N ₂ chamber pressure			
	1.5 MPa	2.0 MPa	2.5 MPa	3.0 MPa
300 °C	carried	carried	carried	carried
350 °C				carried
400 °C				carried
Chamber gas temperature	He chamber pressure			
	1.5 MPa	2.0 MPa	2.5 MPa	3.0 MPa
150 °C		carried		
200 °C	carried	carried	carried	carried
250 °C		carried		
300 °C		carried		

FE-101 stainless steel 316 L					
Chamber gas temperature	N ₂ chamber pressure				
	1.0 MPa	1.5 MPa	2.0 MPa	2.5 MPa	3.0 MPa
200 °C	carried	carried	carried	carried	carried
250 °C	carried	carried	carried	carried	carried
300 °C	carried	carried	carried	carried	carried

Bro-Q and Bro-Atw	
Chamber gas temperature	He chamber pressure
	2.0 MPa
300 °C	carried

The operating gas temperature and pressure conditions in cold spray are shown in Table 4 as to the stainless steel 316 L and bronze powders. The other spray conditions are shown in Table 5. When the deposition efficiency mesurments were carried out, all the substrarate were blasted with alumina grit #36 and the substrate dimensions were 100 x 100 x 5 mm. During the experiments, it was found the the deposition efficiency of MicroMelt powder was extremely low in N₂ gas

process so that He gas process experiments on MicroMelt were added.

The velocity and particle size measurements were carried out without the substrate present. The deposition efficiency of every powder was also measured at every condition shown in Table 4.

Table 5: The cold spray conditions except gas conditions

Stand off distance	20 mm
Torch travers speed	50 mm/sec
Torch travers pitch	1 mm
Powder feed rates	20 g/min

Results and discussions

The cummurative volume fraction as a function of the particle velocity is shown for the two sailless steel powders, MicroMelt and FE-101, and the two bronze powders, Bro-Q and Bro-Atw, in Fig. 4, 5 and 6. The velocity of the angular FE-101 particle is faster than that of the spherical MicroMelt one at the same condition in nitrogen gas process as shown in Fig. 4. The velocity of the spherical particle is about 80 m/sec slower than that of the angular one at 50 % of the volume fraction at the gas pressure of 1.5 MPa and about 100 m/sec slower at 3.0 MPa as shown Fig. 4. The velocity of the spherical particle at 50 % volume fraction at 3.0 MPa in He gas process is almost the same as that of the angular particle at 3.0 MPa in N₂ gas process as shown Fig. 5. The velocity of the spherical Bro-Q particle is also slower than that of the angular Bro-Atw particle at the same spray conditions as shown Fig. 6. The Bro-Q particle velocity is about 60 m/sec slower than the Bro-Atw particle velocity at 50 % of the cumlative fraction even the particle size distributions of Bro-Q are smaller the those of Bro-Atw as shown in Fig. 2.

The fact that the angular particle is more acclerated than the spherical particle in supersonic gas flow suggests the drag coefficient of the angular particle is lager than that of the spherical one. The drag coefficient of a particle is a function of Reynolds and Mach numbers in supersonic gas flow. The drag coefficient increses as Reynolds number decreases. Reynodls number of the angular particle could be smaller than that of the spherical one.

The deposition efficiecies of the stainless steel powders measued in the experiments are shown in Fig. 7. As for the deposition efficiency of the two bronze powders, the results were 28.1 and 89.7 % on Bro-Q and Bro-Atw respectively. As for the staainless steel powders, the deposition efficiency of FE-101 higheer than that of MicroMelt under the same conditions because FE-101 particle had faster velocity than MicroMelt one did as shown Fig. 7.

The deposition efficiency significantly depends on the gas pressure in both N₂ and He gas processes. In N₂ gas process, the deposition efficiency increases as the gas temperature increases. In He gas process, however, the MicroMelt deposition efficiency is little influenced by the temperature.

Assuming that the measured particle velocity without the substrate equals the impact velocity with the substrate palced at the position where the measurements were carried out, if the particle velocity distributions and deposition efficiency are know, the critical velocity can be determined under the assumption that only the particles exceeding the critical velocity can form the deposit on the substrate. When the deposition efficiency is expressed as *DE*, the intersection of

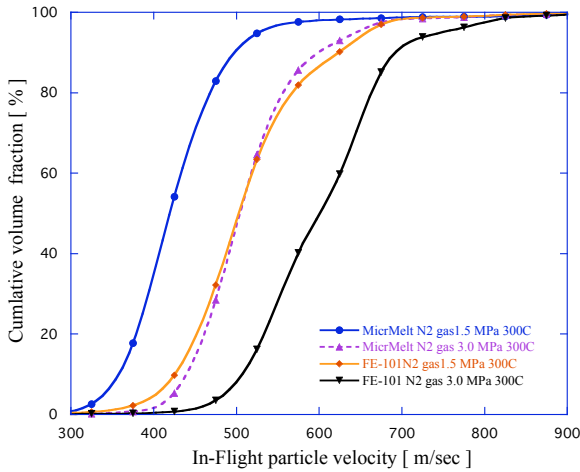


Fig. 4 The cumulative volume fraction of the stainless steel powders as a function of in-flight particle velocity in N₂ gas process.

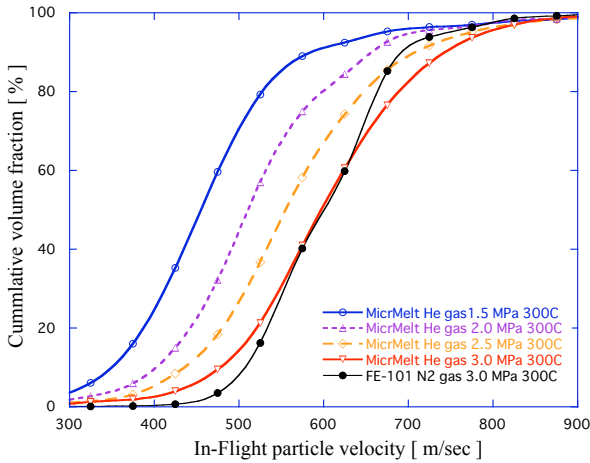


Fig. 5 The cumulative volume fraction of the stainless steel powders as a function of in-flight particle velocity in He gas process.

the cumulative volume fraction curve and $1 - DE$ is the critical velocity. In this way, the critical velocities of every powder under every condition were obtained. The results on the stainless steel powders in N₂ and He gas process are shown in Fig. 8.

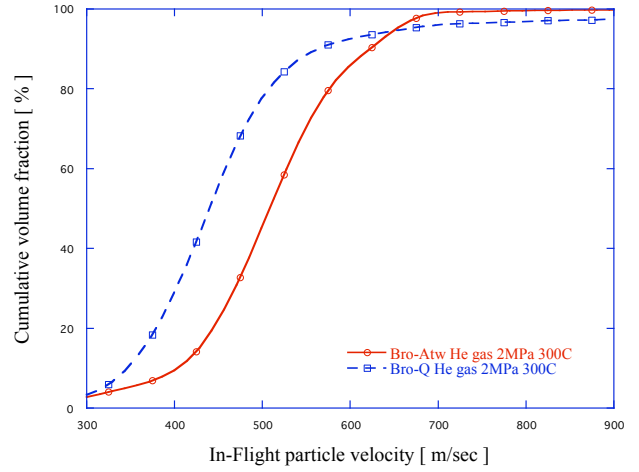


Fig. 6 The cumulative volume fraction of the bronze powders as a function of the particle velocity in He gas process.

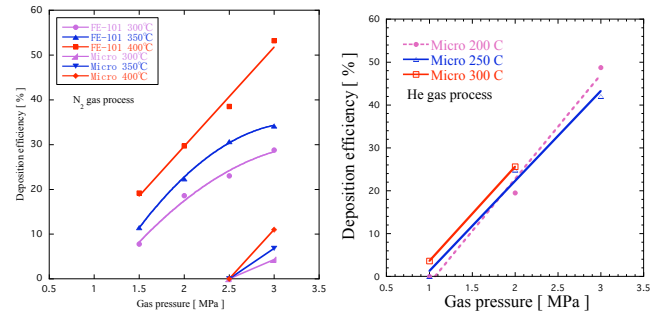


Fig.7 The deposition efficiency of the stainless powders sprayed in N₂ and He gas process.

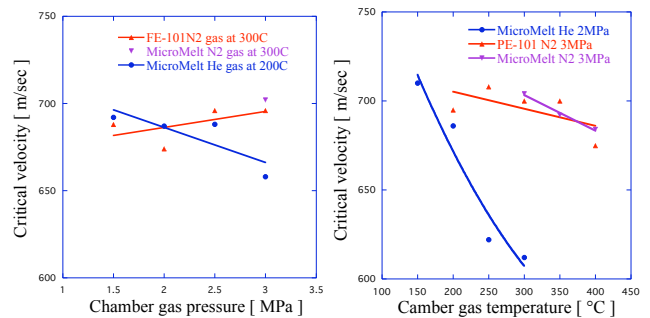


Fig. 8. The critical velocities of MicroMelt powder in both N₂ and He gas processes as a function of the gas pressure or temperature, and the critical velocity of FE-101 powder in N₂ process as a function of the gas pressure or temperature.

In N₂ gas process, the critical velocity of FE-101 powder slightly rises as the pressure increases, only the one value was obtained on critical velocity of MicroMelt powder. Both critical velocity values of MicroMelt and FE-101 are 702 and 695 m/sec respectively at 3.0 MPa of the gas pressure and 300 °C of the gas temperature. The critical velocity values are almost the same. In He gas process, the critical velocity of MicroMelt powder slightly decreases as the gas pressure increases, however it greatly decreases as the temperature rises as shown in Fig. 8. The critical velocity values are in a narrow band between 675 and 710 m/sec except the values at higher gas temperature in He gas process as shown in Fig. 8. The results suggest that the particle hardness did not affect the critical velocity.

The critical velocity values of Bro-Q and Bro-Atw were 486 and 408 m/sec respectively. The higher critical velocity of Bro-Q may be attributed to phosphorus contained in the particle. Phosphorus may make the particle's deformation difficult.

Conclusions

The in-flight particle velocities of the angular particles of both stainless and bronze powders were significantly faster than those of the spherical particles.

The critical velocity values of both the spherical and angular particles were in a narrow band between 675 and 710 m/sec. The particle hardness of the stainless powders did not affect the critical velocity.

The critical velocity of Bro-Q was about 80 m/sec faster than that of Bro-Atw. This may be attributed to phosphorus contained in Bro-Q particle.

The cause that an angular particle is more accelerated than a spherical particle in supersonic gas flow should be clarified in the future study.

References

1. R. C. Dykhuizen and R. A. Neiser, Optimizing the Cold Spray Process, *Thermal Spray 2003: Advancing the Science & Applying the Technology*, 2003, p. 19-24.
2. T. Schmidt, F. Gartner, T. Stoltenhoff, H. Kreye, and H. Assadi, High velocity impact phenomena and coating quality in cold spray, *ITSC 2005: Explore its surfacing potential*, Basel, Switzerland, May, 2005, p. 232-238.
3. J. Voyer, T. Stoltenhoff and H. Kreye, Development of Cold sprayed Coatings, *Thermal Spray 2003: Advancing the Science & Applying the Technology*, 2003, p. 71-78.
4. D. L. Gilmore, R. C. Dykhuizen, R. A. Neiser, T. J. Roeer and M. F. Smith, Particle Velocity and Deposition Efficiency in the Cold Spray Process, *J. Thermal Spray Technology*, Vol. 8 (No.4), 1999, p. 576-582.
5. B. Jodoin, F. Raletz and M. Vardelle, Cold spray modeling and validation, *ITSC 2005: Explore its surfacing potential*, Basel, Switzerland, May, 2005, p. 165-169
6. C.-J. Li, W.-Y. Li, Y.-Y. Wang and H. Fukunuma, Effect of Spray Angle on Deposition Characteristics in Cold Spraying, *Thermal spray 2003: Advancing the Science & Applying the Technology*, Orlando, Florida, USA, May, 2003, p. 91-96.